

An Approach to Estimate Layered Medium by Applying Green's Function to SPAC Method

ZHANG XINRUI & MORIKAWA HITOSHI

Tokyo Institute of Technology, Yokohama, Japan



15 WCEE
LISBOA 2012

SUMMARY:

The underground structure is assumed to be horizontal layers for the spatial auto-correlation method (SPAC), which confines the accuracy of estimation. Hence, we propose a method combining the conventional SPAC method and the concept of Green's function, which is known as seismic interferometry. In this theory, we use the ratio of imaginary part of Green's function at two sites as indicator of the difference of ground structure at corresponding site. SPAC method can provide a rough model of layered medium firstly and the structure is modified to satisfy the ratio of the imaginary part of Green's function. This means that more detailed information of ground structure such as inclination can be obtained by introducing Green's function to SPAC method. We confirm the validity of this method numerically.

Keywords: Green's function, SPAC method, cross spectrum, ground structure, layered medium

1. INTRODUCTION

Since Aki (1957) proposed a new approach to estimate phase velocities of surface waves, spatial auto-correlation (SPAC) method has been a very useful tool to estimate ground structure because of its simple post-process. After that, many researchers both in and out of Japan continued to publish papers on practical adaption of Aki's theory to microtremor exploration. For example, Chavez-Garcia et al. (2006) discussed the validity of performing the SPAC method with a linear array. Morikawa et al. (2004) pointed out that the statistical properties of the spatial autocorrelation function will be independent of the time schedule of the observation at each pair of the sites which improves the application of SPAC method.

However, in all those improved methods, the layers under surface can only be assumed to be horizontal through the SPAC method while in fact, the layers are likely to be inclined slightly with certain angle. Hence, it is expected to obtain more detailed information of ground structure such as inclination by making better use of the records.

In recent years, the seismic interferometry theory (Wapenaar, 2006) has also been widely used to estimate ground structure. It is proved that in an elastic medium the Fourier transform of azimuthal average of the cross correlation of motion between two sites is proportional to the imaginary part of the exact Green's function between these sites (SanchezSesma, 2006 and 2007). Hence, it becomes possible to calculate the ratio of imaginary part of different Green's function by taking the ratio of corresponding cross correlation to analyze ground structure more particularly because Green's function indicates intrinsic property of the medium. In fact, the H/V spectral ratio method has been proved equivalent to the ratio of imaginary part of Green's function in the horizontal and vertical direction, which confirms the feasibility of applying seismic interferometry in frequency domain to microtremor methods. Moreover, seismic interferometry is conditionally consistent with the SPAC method (Yokoi, 2008) which offers the base of introducing seismic interferometry to SPAC method.

SPAC method requires the product calculation of Fourier transformation of records at two sites of center of an array and a one site on the circular array. By taking the ratio of power spectral, we can obtain the ratio of imaginary part of Green's function, respectively, and analyze the difference of ground structure through the ratio. Fig.2.2 shows the image of improvement of the estimation. As for the outline of this

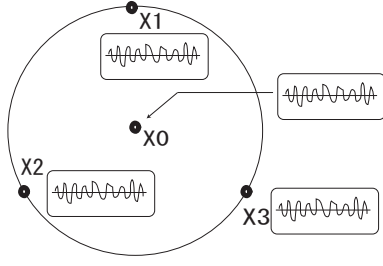


Figure 2.1. The equilateral-triangle array

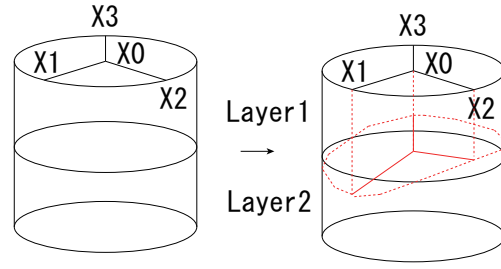


Figure 2.2. An example describing how the new method is expected to raise the accuracy of estimating ground structure.

article, we introduce the necessary fundamental knowledge about SPAC method and seismic interferometry before the new method which combines SPAC method and seismic interferometry is proposed. Then, we confirm the validity of the new method through simulation using finite difference method and discuss its practical significance.

2. THEORETICAL BACKGROUND

In this section, the necessary fundamental knowledge will be introduced including SPAC method and seismic interferometry. It is impossible to demonstrate the two methods very particularly. Only the part, which is applied to the new method, will be explained.

2.1. SPAC Method

Given an equilateral-triangle array and vertical time series records at four sites as Fig.2.1 shows, the azimuthal-average of spatial auto-correlation coefficients $\rho(\omega, r)$ (Aki, 1957) can be calculated as:

$$\rho(\omega, r) = \frac{1}{3} \sum_{j=1}^3 \frac{S_{0j}(\omega)}{S_{00}(\omega)S_{jj}(\omega)}, \quad (2.1)$$

where ω and r are the angular frequency and radius of the circular array, respectively. $S_{jj}(\omega)$ and $S_{0j}(\omega)$ are the power spectra of vertical component of microtremors at site j ($j = 0, 1, 2, 3$) and the cross spectra of the vertical records between site j and 0. The site 0 is center of the array and sites 1, 2, and 3 are located on the circle.

Practically, $S_{jk}(\omega)$ is obtained by the product of Fourier transformation of records at two sites as

$$S_{jk}(\omega) = F(\omega, X_j)F^*(\omega, X_k), \quad (2.2)$$

where X_j is a location of site j and $*$ stands for the complex conjugate. Afterwards, a dispersion curve can be obtained and the property of under-surface layers are estimated using the curve.

2.2. Green's Function from Correlation

It has been demonstrated that in an elastic medium, the averaged cross correlation of motions at sites 1 and 2, whose locations are X_1 and X_2 , can be written as:

$$\langle F_\ell(\omega, X_1)F_m^*(\omega, X_2) \rangle = -2\pi E_s k^{-3} \Im[G_{\ell m}(X_1, X_2, \omega)], \quad (2.3)$$

where ℓ and m indicate one of three directions, (x,y,z). k and E_s are wave number of shear wave and the averaged energy density of shear wave, respectively. $\langle \cdot \rangle$ stands for an expectation and $\Im[\cdot]$ for the imaginary part.

Similar with the SPAC method, many other researchers also has written reports about the retrieval of Green's function by different methods. For example, Wapenaar and Fokkema (2006) has also deduced out the same result as Eqn.2.3 under the different assumption. Normally, it is considered that the assumption of equipartition, i.e., "in the phase space the available energy is equally distributed with a fixed average amount among all the possible states" is necessary for the retrieval of the elastodynamic Green's function from the diffusive wavefield (SanchezSesma, 2006). However, according to the work of Wapenaar and Fokkema (2006), the assumption of uncorrelated point sources with the same power spectra is enough to deduce out Eqn.2.3. The relationship between the two assumptions remains to be discussed. However, it is beyond the scope of this paper. In this article, randomly distributed impulsive sources are used to create diffusive wave field to satisfy Eqn.2.3. More details are interpreted in the next section.

3. A NEW METHOD TO IMPROVE AND ITS VALIDITY

3.1. Combination of SPAC Method and Seismic Interferometry

For the assumed case using an equilateral-triangle array, ℓ and m are both set as vertical direction, which is z , and sites 1 and 2 as the same sites. Hence, Eqn.2.3 yields

$$\begin{aligned} & \langle F_z(\omega, X_1) F_z^*(\omega, X_1) \rangle \\ & = -2\pi E_s k^{-3} \Im[G_{zz}(X_1, X_1, \omega)] \end{aligned} \quad (3.1)$$

Therefore, let us take the ratio of the power spectra at center of the array and an azimuthal site so that the corresponding ratio of imaginary part of Green's function can be obtained as

$$\frac{S_{jj}(\omega)}{S_{00}(\omega)} = \frac{\Im[G_{zz}(X_j, X_j, \omega)]}{\Im[G_{zz}(X_0, X_0, \omega)]} \quad (3.2)$$

and it is expected to analyze the difference of ground structure between every two sites.

In the simplest equilateral-triangle case, three ratios $\frac{S_{11}(\omega)}{S_{00}(\omega)}$, $\frac{S_{22}(\omega)}{S_{00}(\omega)}$, $\frac{S_{33}(\omega)}{S_{00}(\omega)}$ according to Eqn.3.2 can be obtained to analyze the difference between the corresponding two sites. Moreover, it is convenient and efficient to calculate this ratio because the power spectra is just the intermediate result in the process of SPAC method. In order to conform the appropriateness of the proposed method, it is required to see whether Eqn.3.2 works well. Hence, we introduce a model of ground structure and set seismic sources to create certain wavefield numerically and compare the value of left-hand side of Eqn.3.2 with one of right-side. The left-hand side will be calculated using the simulated data and the right-hand side obtained from certain theoretical method.

3.2. Sensitivity analysis for ratio of imaginary part of Green's function

The thickness of each layer is used as the main indicator showing the difference of ground structure at two different sites. If this difference can be identified using the ratio in Eqn.3.2, the estimation of ground structure will be improved as Fig.2.2 shows. Hence, it is required to examine the sensitivity of ratio of imaginary part of Green's function with respect to the difference of thickness.

To confirm it, the right hand side of Eqn.3.2 is calculated theoretically using the method proposed by Hisada (1994 and 1995) for a simple model of ground structure on the basis of the model used in section 3.1. In Hisada's program, we set the delta time to be 0.07s, number of time to be 512 and the maximum frequency to be 5Hz.

We calculate 6 groups of data as shown in Table.3.1. For each group, the ratio of imaginary part of Green's function between Model i ($i=2,3,4,5,6,7$) and Model 1 is calculated in the frequency domain. For example, in Group 1, the thickness of the first layer for Model1 until Model7 is 40,41,42,45,50,55,60 respectively. We calculate out the Green's function of them one by one and take the ratio of that of 41 and 40, 42 and 40, 44 and 40 until 60 and 40. Hence 6 ratios are obtained for each group to see the variation of ratio with the difference of thickness. For Group 1,2 and 3, the difference of thickness among

Table 3.1. Two-layered models of ground structure

Group	Layer	P-wave velocity [m/s]	S-wave velocity [m/s]	Density [t/m ³]	Thickness [m]						
					Models						
					1	2	3	4	5	6	7
1	1	400	70	1.2	40	41	42	45	50	55	60
	2	2000	1000	2.5	∞						
2	1	400	70	1.2	80	81	82	85	90	95	100
	2	2000	1000	2.5	∞						
3	1	400	70	1.2	120	121	122	125	130	135	140
	2	2000	1000	2.5	∞						
4	1	800	400	1.5	40	41	42	45	50	55	60
	2	1800	1200	2.0	∞						
5	1	800	400	1.5	80	81	82	85	90	95	100
	2	1800	1200	2.0	∞						
6	1	800	400	1.5	120	121	122	125	130	135	140
	2	1800	1200	2.0	∞						

models is the same but the starting thickness is different (40m, 80m and 120m) so that the dependance of ratio on the thickness itself can be seen. The group 4,5,6 are under total different model but the setting of thickness is the same as group 1,2,3 so that we can see the variance of the ratio with respect to the property of ground structure. Fig.3.1 shows the ratio of imaginary part of Green's function in frequency domain from group 1 to group 6.

There are totally 6 groups of data. In order to analyze the ratio variation with the thickness more particularly, we take the difference of thickness as one variable ΔD and the frequency which gives the peak value as the function of the variable f_p . Hence, for six groups of data, we can draw six curves in one figure as shown in Fig.3.2.

For each curve of Fig.3.2, the f_p decreases with the ΔD increasing. Hence, for a normal observation of equilateral-triangle array, the thickness difference between each pair of sites can be deduced by comparing the f_p . Comparing among group 1,2,3 or group 4,5,6, it is found that the deeper the second layer is, the smaller the slope will be. It means the sensitivity of ratio with respect to the difference of thickness becomes lower with the depth of the second layer increasing. Hence the new method proposed in this article is more useful to calculate shallow ground structure. Another conclusion is that with the depth of second layer increasing, the ratio becomes smaller. Comparing group 1,2,3 with group 4,5,6, the magnitude of ratio and the f_p depends on factors including the S-wave velocity, P-wave velocity, the average of the layer's thickness of two sites and the difference of the thickness between two sites.

To conform whether there is any relationship between f_p and $\frac{\Delta D}{\bar{D}}$ in which \bar{D} is defined as the average thickness of 2 models:

$$\bar{D} = \frac{D_{Model1} + D_{Modelj}}{2} (j = 2, 3, 4, 5, 6, 7) \quad (3.3)$$

Another figure is drawn as Fig.3.3 shows. It is almost the same as Fig.3.2. Hence, the ratio is not simply dependant on $\frac{\Delta D}{\bar{D}}$.

Anyway, the ratio of imaginary part of Green's function depends on many elements. It is hard to estimate properties of ground structure once from the ratio. However, after obtaining a rough structure by SPAC method which means the S-wave velocity, P-wave velocity and average thickness are known, it becomes easy to estimate more details like ΔD according to the $\Delta D - f_p$ relationships.

3.3. Numerical Simulation for an Inclined Layered Medium

3.3.1. Procedure of the numerical simulation

In this section, the main object is to examine whether the ratio of power spectra and the ratio of imaginary part of Green's function are equal in practice. To make the examination simple, the layered medium is assumed to be 2-layered medium which is linearly and uni-directionally inclined with a small

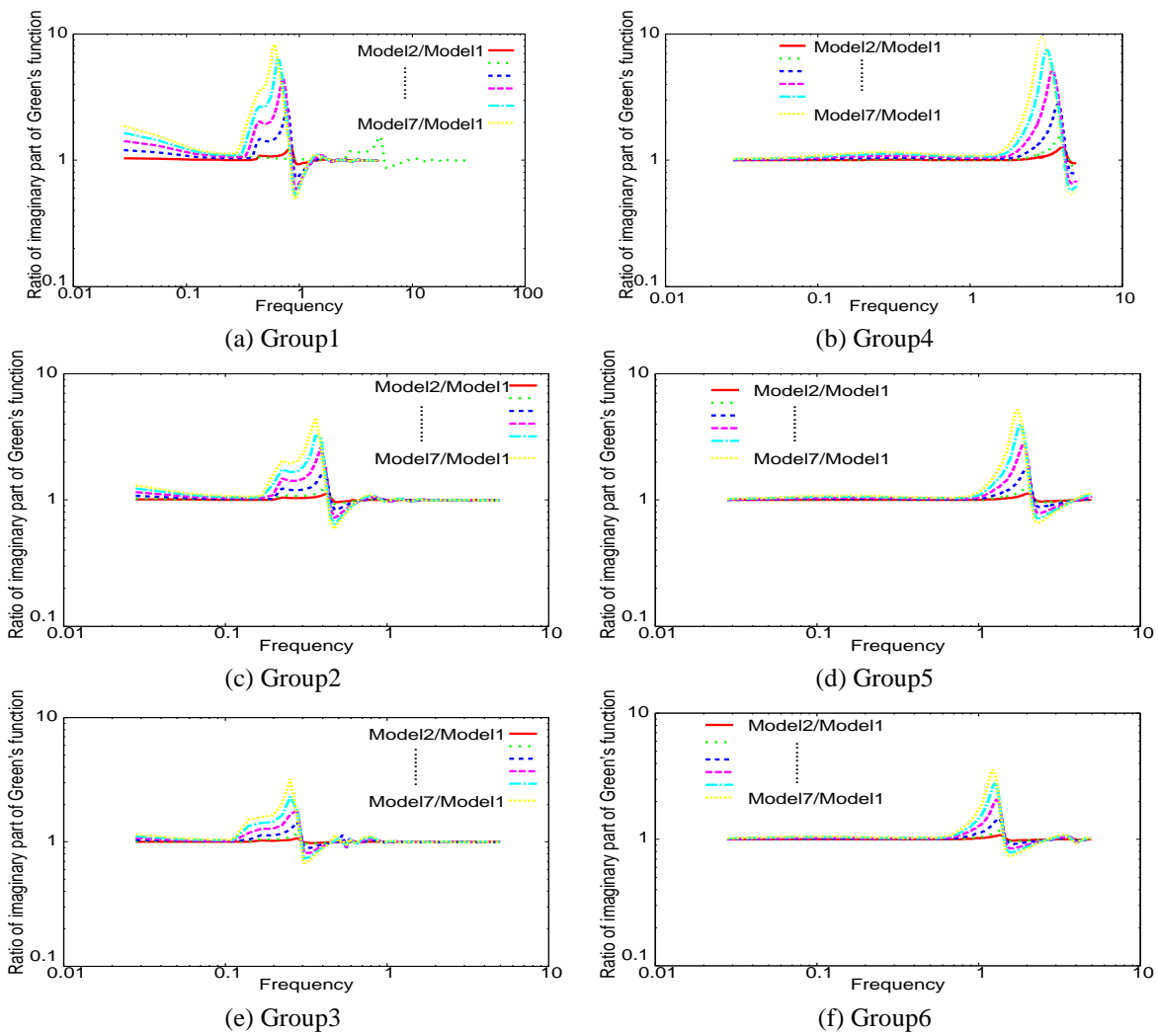


Figure 3.1. The ratio of imaginary part of Green's function between Model 2-7 and Model

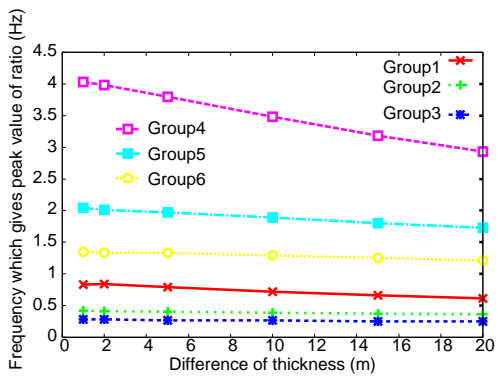


Figure 3.2. Comparison of six groups of data about the $\Delta D - f_p$ relationship

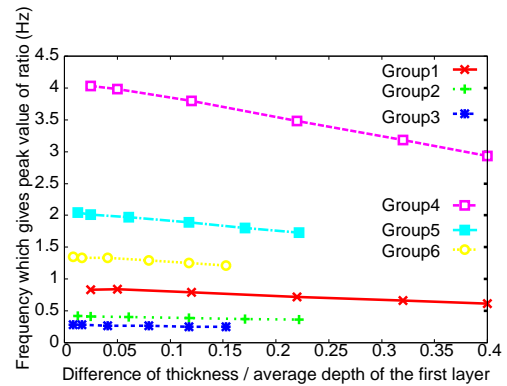


Figure 3.3. Comparison of six groups of data about the $\frac{\Delta D}{D} - f_p$ relationship

angle.

In this case for simplicity, we only observe the vertical part of response wave. In order to simulate proper microtremor wavefield, we also use an impulse force as a source. In order to make the wavefield a diffusive one, random sources with random magnitudes are set at random positions at each timestep. The detailed procedure is shown as below:

Table 3.2. Two-layered models of ground structure (inclined)

Layer	P-wave velocity [m/s]	S-wave velocity [m/s]	Density [t/m ³]	Thickness [m]		
				X1	X2	X3
1	400	70	1.2	44	46	50
2	2000	1000	2.5	∞		

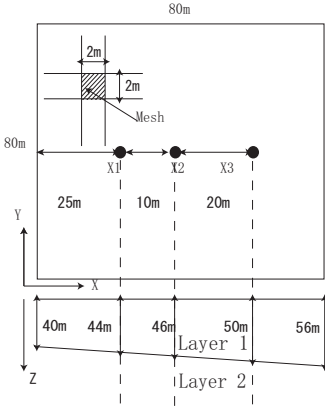


Figure 3.4. Plan and section profile of the layered medium-group 1

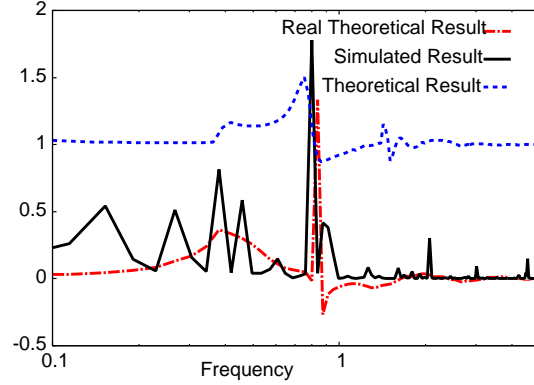


Figure 3.5. One example of comparison among theoretical ratio, simulated ratio and real theoretical ratio

- (1) Generating a random number for number of sources at a specific time.
- (2) Generating random position (X,Y,Z) and magnitude for each source.
- (3) Exerting the sources to the field.
- (4) Update the wavefield for the next time step.
- (5) Repeat step (1)-(4) until over.

According to Yokoi and Margaryan (2008), under these uncorrelated sources, the seismic interferometry is available. This wavefield may not be composed of pure microtremor. However, here the main object is to test the Eqn.3.2.

For each time of calculation, the duration is 120s and the time increment is 0.0008s. Afterwards, we use trapezoidal integration method to transfer the velocity data into displacement data and use FFT method to transform the records in time domain into frequency domain and calculate the power spectra using and take the ratio between some 2 observation sites to compare with the theoretical ratio obtained using Hisada's program.

In order to examine the practical significance of Eqn.3.2, we conduct 6 simple examinations. Similar with the examinations in section 3.2, group 1,2,3 are under the same properties of ground structure. Only the starting thickness is different. Group 4,5,6 are under ground structure with different property. For each group, there are 3 observation sites X1, X2 and X3 which has the different underground structure, namely, the layer's thickness. The spectral ratio between X2 and X1 and the ratio between X3 and X1 is calculated to compare with the theoretical ratio of imaginary part of Green's function.

While all the 6 examinations has been done, Table.3.2 and Fig.3.4 shows the property of layered medium, the plan, the section plan for one examination as an example.

Before discussing the error, it claims attention that in calculating the theoretical Green's function using Hisada's program, we assume the ground structure to be horizontally layered. However, the real ground structure is inclined. This causes the main bias which is simply called assumption bias.

As a simple case to show this bias, we take X1 and X2 in group 1 as example. Instead of calculating Green's function assuming the horizontal layers, we calculate the Green's function of the real inclined layers by exerting the impulsive body force on X1 and calculate the displacement response of X1 according to the definition of Green's function. Then do the same thing to X3 and take the ratio of them to obtain the real theoretical ratio of imaginary part of Green's function. The result is shown in Fig.3.5. We

Table 3.3. Comparison of Theoretical and Simulated f_p for group 1,2,3

X2-X1 (or X3-X1)	46-44	50-44	92-88	100-88	132-128	140-128
Theoretical f_p (Hz)	0.76	0.70	0.39	0.37	0.25	0.25
Simulated f_p (Hz)	0.80	0.79	0.40	0.27	0.23	0.23
Error	0.04	0.09	0.01	0.1	0.02	0.02
Slope	0.011	0.011	0.003	0.003	0.0015	0.0015
Normalised error	1.82	1.36	0.83	2.78	3.33	1.11

Table 3.4. Comparison of Theoretical and Simulated f_p for group 4,5,6

X2-X1 (or X3-X1)	46-44	50-44	92-88	100-88	132-128	140-128
Theoretical f_p (Hz)	3.62	3.42	1.81	1.71	1.26	1.21
Simulated f_p (Hz)	3.33	3.34	2.05	2.04	0.96	0.65
Error	0.29	0.08	0.24	0.33	0.30	0.56
Slope	0.058	0.058	0.016	0.016	0.005	0.005
Normalised error	2.5	0.83	3.75	1.72	15.00	9.33

can see that though the real theoretical ratio matches the result of simulation better, the error of f_p is no much difference for the theoretical one. In practice, it is only available to calculate the theoretical one.

We use the f_p as the indicator of comparison. There are totally 12 comparison between simulated ratio and theoretical ratio. The result is shown in Table.3.3 and Table.3.4.

Except for all the bias, the simulated data at least satisfy all the conclusions drawn in Chapter 3.2: (1) The ratio becomes smaller as the average thickness of two sites becomes bigger. Seeing Table.3.3, the simulated f_p varies from 0.80 to 0.23 as the thickness increases from 45m to 134m. This trend also works in Table.3.4. (2) The ratio becomes smaller as the difference of thickness becomes bigger. Comparing 46 – 44 and 50 – 44, 92 – 88 and 100 – 88, 132 – 128 and 140 – 128, this conclusion can be confirmed. (3) The sensitivity of ratio with respect to the difference of thickness becomes lower with the depth of the second layer increasing.

It is a very good property because using these property, we can at least judge between site 1 and 2 about whose layer is deeper though not knowing the absolute depth.

3.3.2. Error analysis

Though the error can be calculated simply by:

$$E = |\text{Theoretical value} - \text{Simulated value}| \quad (3.4)$$

, it cannot demonstrate the real accuracy of simulated ratio compared with theoretical one because as Fig.3.2 shows, for different average depth, the slope of $\Delta D - f_p$ function is different which means that even if for two situations $E_1 = E_2$, different slope will cause different error of ΔD . Besides, the ΔD is different from each other in the examinations and the error must be compared under the same ΔD because of course bigger ΔD would cause bigger error. Hence we calculate the normalised error:

$$E_n = \frac{E}{S\Delta D} \quad (3.5)$$

as the final indicator of accuracy in which Slope S is simply calculated from Fig.3.2 using

$$S = \frac{\text{First } f_p - \text{Last } f_p}{\text{Last } \Delta D - \text{First } \Delta D} \quad (3.6)$$

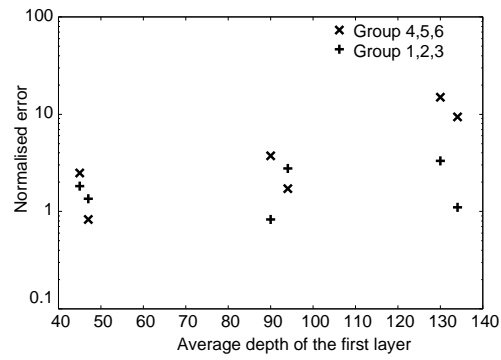


Figure 3.6. The variation of normalised error with respect to the \bar{D}

The normalised errors are shown in Table.3.3 and Table.3.4. Then we see how the new error varies with the average thickness of the first layer by Fig.3.6. Either in the group 1,2,3 or in the group 4,5,6, the error obviously becomes bigger as the second layer becomes deeper. Hence in 2 layered case, the error of the method would be quite big when the depth of second layer is large while the error is small when the depth is small. Hence this method is available in estimating shallow ground structure.

4. CONCLUSIONS

In this article, we discuss the possibility of combining the SPAC method and seismic interferometry to improve the accuracy of estimating layered medium. Accordingly, we try to use the ratio of the power spectra between two different sites to identify the difference of layers' thickness between them. Through theoretical analysis and simulation examination, we draw conclusions as below.

- f_p decreases as ΔD increases. f_p decreases when the second layer becomes deeper. The sensitivity of f_p becomes lower when the second layer becomes deeper. Hence, theoretically, the proposed method is not suitable for deep ground structure.
- As the second layer becomes deeper, the accuracy of simulated ratio becomes worse quickly. Besides, because of the assumption bias, the accuracy cannot be confirmed when the layers are steeply inclined.
- The proposed method is most valid in estimating shallow, slightly-inclined layered medium.

ACKNOWLEDGEMENT

The authors appreciate the valuable discussion with Prof. Hiroyuki Goto of Kyoto University.

REFERENCES

- Aki, K. (1957). Space and time spectra of stationary stochastic waves, with special reference to microtremors, *Bull. Earthq. Res. Inst.*, University of Tokyo, **35**, 415–456.
- Morikawa, H., Sawada, S. and Akamatsu, J. (2004). A method to estimate phase velocity of Rayleigh waves using microtremors simultaneously observed at two sites. *Bulletin of the Seismological Society of America*, **94**, 961-976.
- Chavez-Garcia, F.J., Rodriguez, M. and Stephenson, W.R. (2006). Subsoil Structure using SPAC measurements along a line. *Bulletin of the Seismological Society of America*, **96**, 729-736.
- Wapenaar, K., Draganov, D. and Robertson, J. (2006). Introduction to the supplement on seismic interferometry. *Geophysics*, **71**, SI1eSI 4.
- Sánchez-Sesma, F.J. A theory for microtremor H/V spectral ratio: Application for a layered medium, *Geophysical Journal International*

- Sánchez-Sesma, F.J. and Campillo, M. (2006). Retrieval of the Green's function from cross correlation: The canonical elastic problem, *Bulletin Seismological Society of America*, Vol. 96, No. 3, pp.1182–1191.
- Sánchez-Sesma, F.J., Pérez-Ruiz, J.A., Luzón, F., Campillo, M. and Rodríguez-Castellanos, A. (2008). Diffuse fields in dynamic elasticity, *Wave motion*, **45**, 641-654.
- Yokoi, T and Margaryan, S, (2008). Consistency of the spatial autocorrelation method with seismic interferometry and its consequence, *Geophysical Prospecting*, **56**, 435-451.
- Sakai, Y. (2001). Assess seismic response in high-frequency range of Kyoto Basin using finite difference method.
- Hisada, Y (1994). Efficient method for computing green's functions for a layered half-space with sources and receivers at close depths, *Bulletin of the Seismological Society of America*, **V.84**.
- Hisada, Y (1995). Efficient method for computing Green's functions for a layered half-space with sources and receivers at close depths (Part 2), *Bulletin of the Seismological Society of America*, **V.85**.
- Sakai, K. A method to estimate ground structure with high accuracy applying the combination of microtremor data and gravity data
- Cho, I, Tada, T and Shinozaki, Y. (2006). A generic formulation for microtremor exploration method using three-component records from a circular array, *Geophys. J. Int.*, **165**, 236-258.
- Wapenaar K. and Fokkema J. (2006). Green's function representations for seismic interferometry. *Geophysics*, **71**, SI33-SI46.